Mayer, A.; Roch, T.; Kratz, K.; Lendlein, A.; Jung, F.:

Pro-angiogenic CD14++ CD16+ CD163+ monocytes accelerate the in vitro endothelialization of soft hydrophobic poly(n-butyl acrylate) networks

In: Acta Biomaterialia (2012) Elsevier

DOI: 10.1016/j.actbio.2012.08.011

Pro-angiogenic $CD14^{++}$ $CD16^{+}$ $CD163^{+}$ monocytes accelerate the endothelialisation of elastic hydrophobic poly(*n*-butyl acrylate) networks

Mayer et al. Monocytes support endothelialisation of graft material

Anke Mayer, Toralf Roch, Karl Kratz, Andreas Lendlein, Friedrich Jung

From the Centre for Biomaterial Development and Berlin-Brandenburg Centre for Regenerative Therapies, Institute of Polymer Research, Helmholtz-Zentrum Geesthacht, Teltow, Germany;

Correspondence to Friedrich Jung, Kantstr. 55, 14513 Teltow (E-mail friedrich.jung@hzg.de)

WORD COUNT BODY: 7344

WORD COUNT ABSTRACT: 178

TOTAL NO OF FIGURES & TABLES: 5

KEYWORDS: Biomaterials, endothelialisation, monocytes, small calibre vascular graft, cellular cytokine release system

ABSTRACT

Objective – Overcoming poor endothelialisation of hydrophobic polymer surfaces by co-cultivation of endothelial cells (EC) with angiogenically stimulated intermediate monocytes (aMO2) as a cellular cytokine release system because a functional confluent endothelial cell monolayer on a hydrophobic vascular graft material is crucial for avoiding graft thrombosis.

Methods and results – In the study human umbilical venous endothelial cells or aMO2 in mono- or co-cultures were seeded on poly(*n*-butyl acrylate) networks with an elasticity around 250 kPa. Within three days a functional confluent EC monolayer developed in the co-culture. In contrast the EC in the mono-culture exhibited stress fibres, broadened marginal filament bands and significantly more and larger cell free areas in the monolayer indicating an uncompleted cell-substrate-binding. Remarkably, a monolayer formation could only be achieved in co-cultures, since the addition of recombinant VEGF-A_{165} to the EC mono-cultures did not show this effect.

Conclusion – The study demonstrated the potential of aMO2 as cellular cytokine release system, which adapted their secretion to the demand of EC to generate a functional confluent monolayer on a hydrophobic material intended for small calibre vascular grafts.

Arteriosclerosis is the leading cause of death worldwide. Blood vessel bypassing (CABG) remains the standard treatment especially for end-stage vascular disease. Unfortunately, 40% of patients do not have suitable autologous replacement material.[1] Therefore an increasing need for synthetic vascular grafts must be covered. At present the grafts of choice are made of either PET or ePTFE which both exhibit a satisfying long term patency rate for large calibre grafts (≥ 8 mm) but fail due to their thrombogeneity and intimal hyperplasia as small calibre grafts (< 6 mm). The ideal non-thrombogenic surface is still the native endothelium expressing its glycocalyx.[2] Numerous approaches were performed to establish a functional endothelial cell (EC) monolayer on synthetic materials. Most prominent challenge was thereby the poor EC adhesion. To overcome the problem of poor cell adhesion on polymeric implants, several approaches to support endothelialisation of implant materials were examined during the last decades[3, 4] *in vitro* and *in vivo*: (i) coating with extracellular matrix (ECM) components such as fibronectin, collagen I – IV, vitronectin, laminin, RGDs, and growth factors, (ii) seeding with mesenchymal stem cells, smooth muscle cells, dermal fibroblasts, autologous endothelial cells (EC), and autologous endothelial progenitor cells, (iii) use of biodegradable collagen scaffolds as well as (iv) surface engineering such as the modification of charges, hydrophilicities, and structures. All of those strategies have limitations in successfully establishing a functional confluent EC monolayer on the substrate. The formation of a functional confluent endothelium is described to be dependent on the cytokine milieu of the surrounding environment especially to pro-inflammatory mediators like TNFα[5] and pro-angiogenic growth factors like VEGF-A_{165}.[6] The covalent binding of angiogenic growth factors on the material,[7] the low half-life of growth factors in blood[5] or the dose-dependency of cellular responses[6] might hinder endothelial cell proliferation. As a new strategy in Regenerative Therapies and to achieve haemocompatibility on cardiovascular implants, a specific subset of monocytes might be useful to accelerate the establishment of a functional confluent endothelial cell monolayer on a polymeric surface *in vitro*. Monocytes are circulating leukocytes and key components of the immune system. They are reported in clinical studies to be associated with arteriosclerosis.[8] The morphology, phenotype, and function of circulating peripheral blood monocytes (MO) are heterogeneous. The majority of the MO are characterised as $CD14^{++}$ $CD16^{-}$ and are named “classical” (= MO1).[9] Those MO1 can be activated by lipopolysaccharide and inflammatory cytokines like interferon-γ (IFNγ). They are able to directly kill intracellular pathogens by releasing reactive oxygen species, but can also initiate and modulate T cell responses by antigen presentation and

secretion of inflammatory mediators such as tumor necrosis factor alpha (TNFα), interleukin(IL)-1 beta, IL-6, and IL-12.

Recently, two other subpopulations were described and their nomenclature and functions discussed: $CD14^{++}$ $CD16^{+}$ ("intermediate" = MO2) and $CD14^{+}$ $CD16^{++}$ ("non-classical" = MO3). The latter subpopulation has been already well characterised and is regarded as pro-inflammatory by being a major producer (beside MO1) of the pro-inflammatory TNFα.

MO2 were reported to possess anti-inflammatory properties, but are also associated with angiogenesis and wound healing.[10] Beside CD14 and CD16, MO2 express CD163.[11] CD163 is expressed on pro-angiogenic/anti-inflammatory MO, which are involved in immune regulation by the release of IL-10.

Solely this "intermediate" subset of $CD14^{++}$ $CD16^{+}$ $CD163^{++}$ MO (MO2) secrets VEGF-A_{165} in biologically relevant ranges (>10 ng/ml) after angiogenic stimulation (aMO2) without releasing pro-inflammatory cytokine levels. This had been shown by our group on a glass surface[12] as well as on elastic poly(*n*-butyl acrylate) networks (cP*n*BA)[13] – a candidate material for application as small calibre vascular graft – with E-moduli adjusted to that of human arteries. As biomaterials have to provide mechanical, physiological and biochemical properties similar to those of the surrounding tissues to function properly[14-16] a cP*n*BA network with a Young's modulus of 250 kPa (cP*n*BA0250) was selected (since this modulus is in the range of healthy human arteries which are between 100 kPa[17, 18] and 1000 kPa[19] depending on age and localisation).

Previous studies suggested that aMO2 should be able to mediate the formation of a functional confluent EC monolayer on elastic cP*n*BA substrates.[13, 20] aMO2 continuously secrete growth factors like VEGF-A_{165}, bFGF and PDGF.[13] These as well as other cytokines are the messengers of cell-cell communication[21] regulating the migration and proliferation of EC.[5, 22] The potential adaptive release response of the aMO2 to EC in a co-culture – balancing the cytokine milieu to the demands of the EC at adjusted number of amo2 to EC [bog et al] – might enable this subset of MO to induce a functional confluent EC monolayer on a hydrophobic surface.

To estimate the suitability of aMO2 for supporting the endothelialisation of a hydrophobic elastic biomaterial, EC were cultured on cP*n*BA0250 either under mono-culture conditions or in co-culture with aMO2. Viability, cell density and morphology as well as the cytokine expression profile of the EC on protein as well as on transcriptome level were evaluated. Furthermore, long-term studies were

performed to investigate whether a comparable formation of an EC monolayer could be achieved by daily supplementation with recombinant VEGF-A_{165} in comparison to the aMO2 co-culture.

METHODS

Cells

Charité University Medicine Berlin institutional committee approved experimentation involving human cells.

Primary peripheral blood monocytes (MO) were obtained from healthy donors by density gradient centrifugation as previously described.[12] Briefly, MO were isolated with Monocyte Isolation Kit II (Miltenyi Biotec). Primary $CD14^+$ MO were cultured in ultra-low-attachment dishes in D-MEM and 10% fetal calf serum. Differentiation into intermediate ($CD14^{++}$ $CD16^+$) $CD163^{++}$ MO (MO2) was induced with IL-4 (10 ng/ml) and dexamethasone (100 µM). This was evaluated previously[13] by flow cytometry revealing that ~96% of the $CD14^{++}CD16^+$ MO were positive for CD163. Angiogenic stimulation of MO2 (aMO2) was performed with VEGF-A_{165} (10 ng/ml). Primary human umbilical venous endothelial cells (HUVEC, Lonza) were cultured for no more than 3-5 passages in EGM-2 (Lonza).

Reagents, antibodies, and specimen material

Fluoreszein diacetate (FDA) and propidium iodide (PI) were from Sigma-Aldrich. Antibodies were as follows: Phalloidin-AlexaFluor555® (Invitrogen), anti-human CD14 and CD163 (BD Biosciences), anti-human VE-Cadherin (R&D Systems), and DAPI (Sigma-Aldrich). Round shaped Poly(*n*-butyl acrylate) networks with an *E*-modulus of 250 kPa (cP*n*BA0250) were prepared as previously[23] reported (diameter 13 mm, thickness 1 mm). The endotoxin content of the samples was found to be below 0.5 EU/ml, they did not activate the innate immune system and showed no cytotoxic effects.[24, 25] Before biological tests started, all samples were sterilised by gas sterilisation using ethylene oxide.

Cell culture of aMO2 and HUVEC on cP*n*BA0250

For mono-culture condition 5×10^4 aMO2 or HUVEC were seeded on cP*n*BA0250 in 1 ml EGM-2. For co-culture conditions, 2.5×10^4 aMO2 and 5×10^4 HUVEC were used. After a cultivation time of 3 h, 24 h and 72 h, the viability, morphology, and density (cells per area) of HUVEC, which became adherent to the substrates, were analysed by fluorescent staining and cytokine analysis.

Kinetic comparison study of VEGF-A_{165} gradient and aMO2 co-culture on glass

Glass slides (diameter 13 mm) were seeded with 7.6×10^4 HUVEC in mono-culture or co-cultured with 3.8×10^4 aMO2 in 1 ml EGM-2. EGM-2 was supplemented with either additional 10 ng or 20 ng VEGF-A_{165} per ml and a half medium change performed daily. After 1, 3, 6, 10, 14, 17, and 21 days of cultivation the morphology and number of HUVEC, which became adherent to the substrates, were analysed by fluorescent staining. Supernatants were collected and analysed at each time point. Relative increase of cell density was analysed 1, 2, 3 and 6 days of cultivation using the proliferation assay Click-iT EdU HCS assay from Invitrogen according to manufacturer's protocol. Data were gained with In Cell Analyzer 2000 technology (GE Healthcare Europe) and analysed with In Cell Investigator software (GE). Percentage of relative increase of cell density by proliferation was fluorescently visualised and calculated from sixteen fields per view for each sample at each time point as proliferated cell / total cell number × 100.

Confocal microscopy and immunocytochemistry

To evaluate viability of cells with FDA/PI, 3 µl of FDA stock (5 mg/ml) and 2 µl of PI stock (1 mg/ml) were added directly to the cells 3, 24 and 72 h after seeding on cP*n*BA0250 and incubated for 3 min at 37°C. Percentage of viability was defined to be number of viable cells / total number of cells (viable + dead) × 100. For analysis of cell morphology and density paraformaldehyde-fixed adherent cells on cP*n*BA0250 were first permeabilised with Triton X-100 (0.5 vol%, 10 minutes). Samples were then incubated for 1 hour at 23°C with appropriated antibodies. Confocal microscopy images (five fields of view per sample) were captured using Leica LSM 510 META confocal microscopy. Cell free areas (CFA) within the monolayer after 72 h were sized with the free shape drawing mode of the Axio Vision software.

ELISA

Supernatants from cultured cells were collected and frozen. Concentrations of VEGF-A_{165}, IL-1ra, IL-1β, IL-6, IL-10, IFNγ, and TNFα were evaluated using the Multiplex technique Bio-Plex200® from Bio-Rad Laboratories. MMP activity was determined with pan-MMP fluorogenic peptide substrate Mca-.PLGL-Dpa-AR-NH_2 from R&D Systems. Positive control was recombinant human MMP-9 (R&D Systems). 6-keto Prostaglandin $F_{1\alpha}$ EIA Kit and Thromboxane B_2 EIA Kit were from Cayman Chemical

Company. The assays were performed according to manufacturer's instructions. Samples were run in triplicates.

Reverse transcription and real-time PCR

Total RNA from cells was extracted with the RNeasy mini kit. 100 ng total RNA was used for reverse transcription with Superscript® III reverse transcriptase and oligo dT primers (Invitrogen). RNA and cDNA were quantified with nanodrop (Tecan). Subsequently real time PCR analysis was performed with 100 ng cDNA, using the following primers: VEGF-A_{165}: 5' AGA CCA CTG GCA GAT GTC CC, 3' TGG GCT GCT TCT TCC AAC A; GAPDH: 5' CCA CAT CGC TCA GAC ACC AT, 3' AAA TCC GTT GAC TCC GAC CTT and SYBR green® PCR master mix (Applied Biosystems). The experiments were performed with an Applied Biosystems ABI PRISM® 7500 sequence detection system and specificity of PCR product was determined by melting curve analysis. GAPDH was used as reference gene for normalisation.

Statistics

Data are presented as means ± SD, and statistical significance was determined. Multiple sample tests were performed using one-way analysis of variance (ANOVA). Bonferoni-adjusted p values < 0.05 were considered significant. Prism software was used for statistical analysis.

RESULTS

Cell density, viability and morphology of HUVEC under mono- and co-culture conditions on cP*n*BA0250

HUVEC were sparsely distributed on the cP*n*BA0250 samples 3 h after seeding. The cell numbers per mm^2 did not differ for both culture conditions (mono-culture: 18±5 cells/mm^2; co-culture: 27±9 cells/mm^2, n=6 each). Under both cultivation conditions the EC started to exhibit their typically spread morphology and expressed a physiological actin skeleton (red, Figure 1B and 1C) after 24 h of cell growth. The number of adherent HUVEC per mm^2 increased but did not differ between mono-culture (232±78 cell/mm^2) and co-culture (226±64 cells/mm^2). During the whole experiment under both culture conditions, viability staining indicated that more than 98% of the adherent cells (Figure 1A) were positive for FDA (viable) and negative for PI (dead), demonstrating that neither the culture conditions nor the cultivation on the cP*n*BA0250 samples negatively influenced the number of viable cells.

After 72 h, the majority of the cells were completely spread and the morphology of the HUVEC in the co-culture differed from that of the HUVEC mono-culture. For the aMO2/HUVEC co-culture HUVEC showed a higher density, small marginal filament bands and only few stress fibres (Figure 1C). HUVEC in the mono-culture exhibited a broadened marginal filament bands and a lot of fine and short stress fibres in central parts of the cells. The density of HUVEC in the co-culture system was significantly higher (479±20 cells/mm^2, n=6, $p<0.01$) than in the mono-culture (363±41 cells/mm^2; n=6 each). In the aMO2/HUVEC co-culture, the average cell size seemed to be smaller and cell free areas (CFA) appeared only occasionally in the EC monolayer (9±3 CFA/field of view), while this was significantly more frequent in the HUVEC mono-culture (23±10 CFA/field of view, $p<0.05$). The cell free areas were significantly smaller in the co-culture (175±12 mm^2/sample, 2% of total area, $p<0.05$) compared to the 503±37 mm^2/sample in the HUVEC mono-culture (6% of total area).

Noteworthy, the co-cultured aMO2 were found between the seeded HUVEC three hours after seeding (Fig 1C, white arrows) and, after reaching confluence (72 h after seeding), all aMO2 were situated only on top of the HUVEC monolayer and were not incorporated or located below. The aMO2 did not form clusters during the whole observation period (72 h) and they were equally distributed over the complete HUVEC monolayer.

Cytokine secretion analysis of aMO2 and/or HUVEC on cP*n*BA0250

The mean VEGF-A_{165} concentration of aMO2 cells (6.05±0.20 ng/ml) cultivated for 3 h was comparable to VEGF-A_{165} in HUVEC mono- and co-culture (5.95±0.28 ng/ml HUVEC alone, 5.96±0.22 ng/ml HUVEC co-culture). However, the VEGF-A_{165} concentration was significantly increased in aMO2 mono-culture 24 h after seeding (p<0.001, 11.14±1.00 ng/ml) but was not significantly different in the supernatant of HUVEC, which were cultured alone (5.44±0.18 ng/ml) compared to the amount in the supernatant of HUVEC and aMO2 cultured together (5.61±0.15 ng/ml). The VEGF-A_{165} concentration of aMO2 mono-culture was decreased after 72 h (7.83±0.51 ng/ml). Nevertheless, in both HUVEC cultures (with and without aMO2) the measured VEGF-A_{165} concentrations were decreased 72 h after seeding and significantly less than in the supernatant of aMO2 mono-culture (p<0.001, HUVEC mono-culture: 0.04±0.02 ng/ml, HUVEC/aMO2 co-culture: 0.08±0.01 ng/ml).

The secretion levels of the pro-inflammatory cytokines IL-1β, IL-6, IFNγ, and TNFα were very low (< 3 pg/ml) in the aMO2 mono-culture and the aMO2/EC co-culture. In contrast, the secretion of TNFα (14 – 16 pg/ml) and IL-6 (18 – 19 pg/ml) was significantly higher (p<0.01) in the EC mono-culture and IL-1β similar to the aMO2 cultures within the first 24 h. The amounts of the pro-inflammatory cytokines in the EC mono-culture were equally low as in the aMO2 mono-culture and in the aMO2/EC co-culture 72 h after seeding.

Besides VEGF-A_{165} only two anti-inflammatory cytokines, IL-1ra and IL-10, were detectable but still <200 pg/ml: 38 – 58 pg/ml for IL-10 and 53 – 137 pg/ml for IL-1ra. The values of those cytokines were comparable for both HUVEC cultures over time.

MMP activity of aMO2 and/or HUVEC on cP*n*BA0250

The addition of aMO2 to HUVEC did not change the MMP activities in the cell culture supernatants, since HUVEC mono-cultures displayed a similar FI. In contrast aMO2 showed a significantly lower activity of MMPs (p<0.001) on cP*n*BA0250 at 24 h and 72 h compared to HUVEC mono- and co-cultures (Figure 2B).

mRNA expression of VEGF-A_{165} in HUVEC and/or aMO2 cultures on cP*n*BA0250

The VEGF-A_{165} mRNA expression of aMO2 remained stable and was significantly higher than in HUVEC co- and mono-culture (p<0.01, data not shown).

The VEGF-A_{165} mRNA expression of the HUVEC mono-culture decreased over time from 0.006±0.002 (3 h) to 0.002±0.001 (-67%, p<0.05, 24 h) and remained almost constant until the end of the experiment 72 h after seeding (Fig 2A).

When HUVEC were co-cultured with aMO2 for 3 h, the VEGF-A_{165} mRNA expression (0.010±0.005) was increased compared to the transcriptome level of the HUVEC mono-culture (p<0.05). After 24 h of co-cultivation, the relative mRNA expression level of VEGF-A_{165} was 0.007±0.005 and was still significantly higher than in the HUVEC mono-culture despite the reduction (p<0.01). At the end of the cultivation time period the VEGF-A_{165} mRNA expression decreased further in the co-culture to 0.002±0.001 thereby assimilating to the transcriptome level of the HUVEC mono-culture. So the overall decrease in the HUVEC/aMO2 co-culture was 81% within 72 h (p<0.05).

Cell density, morphology and proliferation of HUVEC under mono-culture conditions with and without VEGF-A_{165} or in co-culture with aMO2 on glass over 21 days

In order to evaluate whether a VEGF-A_{165} supplementation can also accelerate the endothelialisation or might lead to disoriented overgrowth, HUVEC were cultured with additional 10 ng/ml or 20 ng/ml VEGF-A_{165} and compared to HUVEC cultures or to co-cultures with aMO2. For this study glass was used to provide HUVEC optimal conditions: HUVEC adhere, migrate and proliferate better on glass than on cP*n*BA0250, in addition, glass does not adsorb as much VEGF-A as cP*n*BA0250.

After one day of seeding, the cell density of adherent cells was significantly higher when HUVEC were cultured in medium supplemented with VEGF-A_{165} (10ng: 35±13 cells/mm^2, 20ng: 48±14 cells/mm^2) or co-cultured with aMO2 (51±16 cells/mm^2) than cultured separately in regular EGM-2 (19±6 cells/mm^2, p<0.01). This trend remained until day 14 (Table 1). At day 17 the cell density of adherent cells was highest when HUVEC were cultured with additional 20 ng/ml VEGF-A_{165} (523±73 cells/mm^2) or in presence of aMO2 (459±77 cells/mm^2). Cell numbers of HUVEC cultivation in EGM-2 without additional VEGF-A_{165} or supplemented with 10 ng/ml VEGF-A_{165} were significantly lower and comparable to each other (Table 1). On day 21 for all three HUVEC mono-cultures the cell number decreased comparable to that of day 10 and were significantly lower than in the HUVEC/aMO2 co-culture (p<0.01).

The morphology of HUVEC was similar in all four cultures until day 1. Although the average cell density of adherent cells increased over time with additional VEGF-A_{165} supplementation, plaques of cells detached and were washed away during the staining procedure. Representative pictures are

shown in Figure 6. In those VEGF-A_{165} supplemented HUVEC presence of stress fibres and only scattered marginal filaments were observed (as also shown in Figure 1C). In contrast when HUVEC were co-cultured with aMO2, the cell density of adherent cells was not only significantly increasing but the distribution of the cells also remained consistent, filaments networks were prominent in the margin of the cell, and stress fibres were absent. At day 10 of cultivation the number of adherent HUVEC in the VEGF-A_{165} supplemented cultures reached the numbers of the co-cultured cells but was still below their level with different filament networks and bigger cell size. Until the end of the experiment the growth kinetic of the cultures revealed that the highest cell density with marginal filament networks and absent stress fibres was gained when HUVEC were co-cultured with aMO2. However, the increase in cell number was higher when VEGF-A_{165} was added to the culture medium but this progression switched completely ending in lower or similar numbers and density compared to the control culture.

The proliferation rate of HUVEC under all four culture conditions was comparable at all time points. Only at day 3 the proliferation rate of HUVEC co-cultured with aMO2 was significantly lower (p<0.05, 35.8±13.6 %) than in the HUVEC mono-cultures in EGM-2 medium with or without additional VEGF-A_{165} supplementation (Supplemental Table 1).

PGI2 and TXB2 secretion analysis of HUVEC under different culture conditions with and without VEGF-A_{165} or co-cultured with aMO2 on glass over 14 days

The dynamic of PGI2 secretion was in the co-culture similar to that of the EGM-2 control culture while in the VEGF-A_{165} supplemented cultures the secretion dynamic differed (Table 2A).

During the first three days of cultivation, the secreted amounts of the vasoconstrictor TXB2 in the control culture and the HUVEC/aMO2 co-culture were comparable whereas in both VEGF-A_{165} supplemented cultures more TXB2 was found. Although the secretion of TXB2 increased in the following days until the end of the experiment (Table 2B) the measured values remained in the very low picogram range. The increase pattern was comparable for all 4 culture conditions.

MMP activity of HUVEC cultured with and without additional VEGF-A_{165} or in co-culture with aMO2 on glass over 14 days

When HUVEC were cultured in regular EGM-2 for 1 and 3 days, their MMP activity was significantly higher (p<0.05, Supplemental Figure 1) than the activity of HUVEC cultured with either 10 ng/ml VEGF-A_{165}, 20 ng/ml VEGF-A_{165} or aMO2. At day 6 of cultivation the MMP activities in all 4 cultures

were comparable. However, after 10 days of cultivation the MMP activity of the VEGF-A_{165} supplemented or with aMO2 co-cultured HUVEC was significantly increasing (aMO2 co-culture: p<0.01; VEGF-A_{165} supplemented: p<0.001) while the MMP activity of the HUVEC control decreased. At day 14 the MMP activity of the HUVEC control increased to a comparable level of the aMO2/HUVEC culture whereas the MMP activity of VEGF-A_{165} supplemented HUVEC was again significantly increasing (p<0.001) with highest activity in HUVEC cultured with 20 ng/ml VEGF-A_{165} supplementation.

VE-Cadherin expression of HUVEC mono-culture on cP*n*BA0250 or glass

On cP*n*BA0250 VE-Cadherin was not found in the border areas of HUVEC (Figure 7 A) as generally found on glass (Supplemental Figure 2). The lower part of Figure 7 A showed a high migration activity of HUVEC. The VE-Cadherin was not cumulated in the cell border areas but diffusely spread across the cell typical for the subconfluent state of strongly migrating cells [26].

DISCUSSION

To our knowledge, no studies were performed using autologous immune cells like aMO2 as a cellular cytokine release system to support the endothelialisation of biomaterials. Mammalian cells generally interact better with hydrophilic surfaces than with hydrophobic surfaces[27] what impedes the endothelialisation of hydrophobic biomaterials. Only in case of co-cultivation with aMO2, functional confluent EC monolayers on the hydrophobic cP*n*BA0250 were achieved with cell densities nearly comparable to EC densities *in vivo* [28] and which are assumed to be needed for a long-term patency of synthetic vascular grafts *in vivo*.[29] These EC showed a small marginal filament band without stress fibres as found *in situ* so that only for the co-cultured EC a functional confluent EC monolayer can be considered.[30]

HUVEC mono-cultures on cP*n*BA0250 revealed a distinct stress fibre formation which is described to play a crucial role in binding EC to the substrate.[30] They are mainly found during migration, in response to shear load[30] and after milieu changes.[31]

Such stress fibres were not found when HUVEC were co-cultured with aMO2, what probably might be due to the cytokine milieu given by the aMO2, which not only provided VEGF-A_{165} but also the growth factors (GFs) bFGF and PDGF-BB[13] and anti-inflammatory cytokines like IL-1ra and IL-10. Those factors are known to be important for the maturation and stabilisation of newly build EC monolayers.[32]

Co-cultured aMO2 settled between HUVEC within the first 24 h. After a HUVEC confluence of nearly 90% was reached, all aMO2 were situated on top of the monolayer but not incorporated or below the endothelial layer (Figure 3). This differs from the *in vivo* situation where MO can infiltrate through the EC monolayer[33] differentiating into dendritic cells (DCs) by re-entering the vessel.[34] This differentiation into DCs mainly occurs during inflammation and in presence of pro-inflammatory cytokines such as IL-6,[34] which could not be detected in our experiment. The cytokine profile measured excluded a differentiation of the aMO2 into DCs during the endothelialisation of cP*n*BA0250. The self-adjusting homogeneous distribution of the aMO2 between the EC (later on top of the EC) may result in a consistent local concentration of cytokines and GFs by diffusion supporting a uniform migration and proliferation of the EC. This widespread distribution avoided a focal excessive proliferation of EC due to an unbalanced GF distribution as it may occur from local active agent depots of implanted devices.[35]

The VEGF-A_{165} concentrations of HUVEC within the first 24 hours were comparable. However, after 72 hours, although markedly decreased, the supernatant of the HUVEC/aMO2 co-culture contained twice as much VEGF-A_{165} (p<0.01) than the HUVEC mono-culture supernatant. The presence of the aMO2 might have induced an increased HUVEC proliferation resulting in a significantly higher number of EC after 72 h of cultivation. The occurring VEGF-A_{165} during the proliferation might entail a further stimulation of the aMO2 to secrete even more VEGF-A_{165} thereby again stimulating HUVEC resulting in a positive feedback loop. The evaluation of the transcriptome levels of VEGF-A_{165} over time in the HUVEC mono-culture and HUVEC/aMO2 co-culture supported this suggestion. These results support the hypothesis of an intercellular communication between EC and aMO2 resulting in a secretion of cytokines by the aMO2 adapted to the demand of EC.

The amounts of the cytokines IL-1β, IL-1ra and IL-10 were comparable and clearly below biologically effective thresholds for all cell culture setups. TNFα and IL-6 were significantly higher (p<0.01) in the HUVEC mono-culture than in the aMO2 mono- or co-culture. This indicated that the aMO2 remained in their status and did not switch into MO1 or MO3 status and also reduced the stress-dependent release of those cytokines by HUVEC.

The matrix metalloproteinase (MMP) activity of aMO2 adhering on cP*n*BA0250 was very low and stable over time. This is extremely important because an elevated MMP production could cause the degradation of ECM[36] or promote caspase-mediated death of EC.[37, 38] On the other hand, a controlled ECM remodelling is necessary for migration and proliferation of vascular cells as well as the elasticity

of the vessels.[39] As the MMP activity of HUVEC in the co-culture was comparable to the MMP activity in the HUVEC mono-culture the aMO2 seem not to influence the MMP activity of the HUVEC. These results indicated that HUVEC remained in their quiescent physiological status as well as the cytokine profile and the low MMP activity of the aMO2 confirmed that the aMO2 did not switch into MO1 or MO3 status.[40]

As isolation and enrichment of aMO2 is time consuming,[41] therefore we examined in a supplementary long-term study (21 days) whether a manual supplementation of the HUVEC culture with recombinant VEGF-A_{165} can result in a functional confluent EC monolayer also.

Until today, different approaches are explored in order to support endothelialisation of biomaterial surfaces by angiogenic growth factors like VEGF. In the 1990´s most materials were just incubated in GF solutions binding GFs to the material surface by adsorption.[42] But with a VEGF half-life time of approximately 3 min in blood[5] the adsorbed GFs disappear within 1 hour from the surface. Recent approaches as immobilisation of GFs by covalent binding on the material carry a strong possibility of altering the GF bioactivity[7] as well as the interaction with its cell receptor. A further problem might occur by the potential for ultraviolet-induced damage to the GF.[43] In addition, present studies showed that immobilised GFs dramatically limited the cellular responses,[44] especially their proliferation.[45]

To overcome an eventual limited bioactivity of bound GFs the cell cultures were manually supplemented with VEGF-A_{165} daily. The results revealed that the average numbers of HUVEC were significantly higher when VEGF-A_{165} was added (10 ng/ml and 20 ng/ml respectively) daily. But compared to HUVEC of the aMO2 co-culture the established EC monolayer was less adherent. Not before day 21 – despite daily VEGF-A_{165} supplementation – was any confluent EC monolayer established. The EC number was increasing but the cell-cell-contacts seemed not to be completely functional so that at different time points new gaps (intercellular fenestrations) in the monolayer arose while other denuded areas healed (Figure 3). Despite comparable EC proliferation since cultivation day 3 for all four culture conditions the cell densities in the VEGF-A_{165} supplemented cultures were lower than in the co-culture. This seemed to be caused by the detachment of single cells and cell groups confirmed by the development of new cell free areas during the whole study period. The indication of incomplete cell-cell-binding was strengthened by the broadening of the marginal filament bands and the appearance of stress fibres in central parts of the cells. VEGF-A_{165} is reported to increase migration of EC associated with the loss of VE-Cadherin in the border area of the cells.[46] To

enable the cell to migrate, the adherence is impaired by internalising VE-Cadherin thereby loosening the cell-cell-binding.[46] Probably this VE-Cadherin dependent impairment led to the intercellular fenestrations ("denuded areas") in the VEGF-A_{165} supplemented mono-cultures, which were not observed in the aMO2 co-culture.

The proliferation rate differed between the three HUVEC mono-cultures and the aMO2/HUVEC co-culture. In those HUVEC mono-cultures with different VEGF-A_{165} supplementation on glass, the maximum of proliferation was reached at day 3 and then declined whereas the proliferation rate of the co-culture rose comparably until day 2 and then remained almost constant. At day 3 of cultivation the co-culture proliferation rate was significantly ($p<0.05$) lower as in the 3 HUVEC mono-cultures. Nevertheless only in the co-culture a higher cell density and an earlier confluence was detected obviously due to the better adherence of HUVEC within the first 24 hours. The aMO2 seemed to provide a more physiological and gentle culture milieu[47] resulting in a more physiological cell behaviour and appearance of the HUVEC. It is noteworthy to point out that these results were attained only with a ratio of one aMO2 for two EC which had been figured out in a former pilot study.[48]

The secretion of prostacyclin (PGI2) showed a decreasing trend with increasing incubation time while thromboxane (TXB2) slightly increased. The production of these two compounds is very well balanced under physiological conditions[49, 50] and discussed as the responsible mechanism for the maintenance of vascular homeostasis.[51] As PGI2 is the most potent inhibitor of platelet aggregation as well as a vasodilator and TXB2 is its potent antagonist, this PGI2 reduction might indicate that HUVEC were slightly activated over time.[52] Although this PGI2 decrease was found in the co-culture as well as in the 3 HUVEC cultures, the dynamic pattern of PGI2 in the co-culture was comparable to that of HUVEC culture without supplementation of additional VEGF-A_{165}. This observation might explain why in the EC monolayer of VEGF-A_{165} supplemented cultures detachment of HUVEC occurred (Figure 6) while this was not the case for the EC monolayer of the aMO2/HUVEC co-culture. Obviously, the aMO2 influenced the release of active substances secreted by EC. It is shown, that activated EC secrete more than 600 mostly unknown polypeptides/proteins[53] which seemed to lack in the VEGF-A_{165} treated HUVEC. This can be regarded as a further proof that GF supplementation alone is not sufficient and a specific cocktail of cytokines, GFs and further probably unknown factors is needed for a balanced and successful endothelialisation. The aMO2 seem to posses the ability to provide this cocktail in an adaptive manner.

In conclusion, the study demonstrated the potential of aMO2 as cellular cytokine release system, which adapt their secretion to the demand of EC to generate a functional confluent monolayer on an elastic hydrophobic polymer aimed for the application as small calibre vascular graft. Only a co-culture with aMO2, but not a supplementation with recombinant VEGF-A_{165} provided sufficient support for the formation of a functional confluent EC monolayer without negatively influencing the envisioned EC monolayer (e.g. formation of stress fibres) or the environmental milieu (e.g. pro-inflammatory cytokines).

SOURCES OF FUNDING

The study was supported by the Berlin-Brandenburg Center for Regenerative Therapies – BCRT (Helmholtzförderung, Impuls- und Vernetzungsfond: SO-036) and by the Twinning grant: "Novel strategies for vascular regeneration after coronary interventions based on vascular healing drugs, improved stent hemocompatibility and pre-determined drug-release" from the BCRT.

DISCLOSURES

None

REFERENCES

1. Faries PL, Logerfo FW, Arora S, Pulling MC, Rohan DI, Akbari CM, Campbell DR, Gibbons GW, Pomposelli FB, Jr. Arm vein conduit is superior to composite prosthetic-autogenous grafts in lower extremity revascularization. *J Vasc Surg*. 2000;31:1119-1127
2. Broekhuizen LN, Mooij HL, Kastelein JJ, Stroes ES, Vink H, Nieuwdorp M. Endothelial glycocalyx as potential diagnostic and therapeutic target in cardiovascular disease. *Curr Opin Lipidol.* 2009;20:57-62.
3. Chlupac J, Filova E, Bacakova L. Blood vessel replacement: 50 years of development and tissue engineering paradigms in vascular surgery. *Physiol Res*. 2009;58 Suppl 2:S119-139
4. Hoenig MR, Campbell GR, Rolfe BE, Campbell JH. Tissue-Engineered Blood Vessels. *Arterioscler Thromb Vasc Biol*. 2005;25:1128-1134
5. Folkman J. Angiogenesis in cancer, vascular, rheumatoid and other disease. *Nat Med.* 1995;1:27-31
6. Akeson A, Herman A, Wiginton D, Greenberg J. Endothelial cell activation in a VEGF-A gradient: Relevance to cell fate decisions. *Microvasc Res*. 2010;80:65-74
7. Masters KS. Covalent Growth Factor Immobilization Strategies for Tissue Repair and Regeneration. *Macromol Biosci*. 2011:1149-1163
8. Nasir K, Guallar E, Navas-Acien A, Criqui MH, Lima JA. Relationship of monocyte count and peripheral arterial disease: results from the National Health and Nutrition Examination Survey 1999-2002. *Arterioscler Thromb Vasc Biol*. 2005;25:1966-1971
9. Ziegler-Heitbrock L, Ancuta P, Crowe S, Dalod M, Grau V, Hart DN, Leenen PJ, Liu YJ, MacPherson G, Randolph GJ, Scherberich J, Schmitz J, Shortman K, Sozzani S, Strobl H, Zembala M, Austyn JM, Lutz MB. Nomenclature of monocytes and dendritic cells in blood. *Blood*. 2010;116:74-80
10. Skrzeczyńska-Moncznik J, Bzowska M, Lo˝seke S, Grage-Griebenow E, Zembala M, Pryjma J. Peripheral Blood CD14high CD16+ Monocytes are Main Producers of IL-10. *Scand J Immunol*. 2008;67:152-159
11. Buechler C, Ritter M, Orso E, Langmann T, Klucken J, Schmitz G. Regulation of scavenger receptor CD163 expression in human monocytes and macrophages by pro- and antiinflammatory stimuli. *J Leukoc Biol*. 2000;67:97-103
12. Mayer A, Lee S, Jung F, Grütz G, Lendlein A, Hiebl B. CD14+ CD163+ IL-10+ monocytes/ macrophages: Pro-angiogenic and non pro-inflammatory isolation. *Clin Hemorheol Microcirc*. 2010;46:217-223
13. Mayer A, Kratz K, Hiebl B, Lendlein A, Jung F. Interaction of angiogenically stimulated intermediate CD163+ monocytes/macrophages with soft hydrophobic poly(*n*-butyl acrylate) networks with elastic moduli matched to that of human arteries. *Artif Organs*. 2011;DOI:10.1111/j.1525-1594.2011.01410.x
14. Wood JA, Shah NM, McKee CT, Hughbanks ML, Liliensiek SJ, Russell P, Murphy CJ. The role of substratum compliance of hydrogels on vascular endothelial cell behavior. *Biomaterials*. 2011;32:5056-5064
15. Shastri VP, Lendlein A. Materials in Regenerative Medicine. *Adv Mat*. 2009;21:3231-3234
16. Lee S, Lee RT. Mechanical Stretch and Intimal Hyperplasia. *Arterioscler Thromb Vasc Biol*. 2010;30:459-460
17. Patel DJ, Janicki JS, Carew TE. Static anisotropic elastic properties of the aorta in living dogs. *Circ Res*. 1969;25:765-779
18. Patel DJ, Janicki JS. Static elastic properties of the left coronary circumflex artery and the common carotid artery in dogs. *Circ Res*. 1970;27:149-158

19. Riley WA, Barnes RW, Evans GW, Burke GL. Ultrasonic measurement of the elastic modulus of the common carotid artery. The Atherosclerosis Risk in Communities (ARIC) Study. *Stroke*. 1992;23:952-956
20. Mayer A, Hiebl B, Lendlein A, Jung F. Support of HUVEC proliferation by pro-angiogenic intermediate CD163+ monocytes/macrophages: A co-culture experiment. *Clin Hemorheol Microcirc*. 2011;49:423-430
21. Balkwill FR. *The cytokine network*. Oxford; New York: Oxford University Press; 2000.
22. Kurogane Y, Miyata M, Kubo Y, Nagamatsu Y, Kundu RK, Uemura A, Ishida T, Quertermous T, Hirata K-i, Rikitake Y. FGD5 Mediates Proangiogenic Action of Vascular Endothelial Growth Factor in Human Vascular Endothelial Cells. *Arterioscler Thromb Vasc Biol*. 2012;32:988-996
23. Cui J, Kratz K, Hiebl B, Jung F, Lendlein A. Soft poly(n-butyl acrylate) networks with tailored mechanical properties designed as substrates for in vitro models. *Polym Adv Technol*. 2011;22:7
24. Roch T, Cui J, Kratz K, Lendlein A, Jung F. Immuno-compatibility of soft hydrophobic poly(n-butyl acrylate) networks with elastic moduli for regeneration of functional tissues. *Clin Hemorheol Microcirc*. 2011;DOI: 10.3233/CH-2010-1449
25. Hiebl B, Cui J, Kratz K, Frank O, Schossig M, Richau K, Lee S, Jung F, Lendlein A. Viability, Morphology and Function of Primary Endothelial Cells on Poly(n-Butyl Acrylate) Networks Having Elastic Moduli Comparable to Arteries. *J Biomater Sci Polym Ed*. 2011: Epub Mar 31, DOI:10.1163/092050611X092566144
26. Dejana E. Endothelial cell-cell junctions: happy together. *Nat Rev Mol Cell Biol*. 2004;5:261-270
27. Grinnell F, Milam M, Srere PA. Studies on cell adhesion. II. Adhesion of cells to surfaces of diverse chemical composition and inhibition of adhesion by sulfhydryl binding reagents. *Arch Biochem Biophys*. 1972;153:193-198
28. Fadini GP, Avogaro A. Cell-based methods for ex vivo evaluation of human endothelial biology. *Cardiovasc Res*. 2010;87:12-21
29. Deutsch M, Meinhart J, Fischlein T, Preiss P, Zilla P. Clinical autologous in vitro endothelialization of infrainguinal ePTFE grafts in 100 patients: a 9-year experience. *Surgery*. 1999;126:847-855
30. Franke RP, Grafe M, Schnittler H, Seiffge D, Mittermayer C, Drenckhahn D. Induction of human vascular endothelial stress fibres by fluid shear stress. *Nature*. 1984;307:648-649
31. Liu SM, Sundqvist T. Effects of hydrogen peroxide and phorbol myristate acetate on endothelial transport and F-actin distribution. *Exp Cell Res*. 1995;217:1-7
32. Hao X, Månsson-Broberg A, Gustafsson T, Grinnemo KH, Blomberg P, Siddiqui AJ, Wärdell E, Sylvén C. Angiogenic effects of dual gene transfer of bFGF and PDGF-BB after myocardial infarction. *Biochem Biophys Res Commun*. 2004;315:1058-1063
33. Takahashi M, Masuyama J-I, Ikeda U, Kitagawa S-I, Kasahara T, Saito M, Kano S, Shimada K. Suppressive Role of Endogenous Endothelial Monocyte Chemoattractant Protein–1 on Monocyte Transendothelial Migration In Vitro. *Arterioscler Thromb Vasc Biol*. 1995;15:629-636
34. Chomarat P, Banchereau J, Davoust J, Karolina Palucka A. IL-6 switches the differentiation of monocytes from dendritic cells to macrophages. *Nature Immunol*. 2000;1:510-514
35. Amsden BG. Delivery approaches for angiogenic growth factors in the treatment of ischemic conditions. *Expert Opin Drug Deliv.* 2011;8:873-890
36. Newby AC. Dual role of matrix metalloproteinases (matrixins) in intimal thickening and atherosclerotic plaque rupture. *Physiol Rev*. 2005;85:1-31

37. Lee SR, Lo EH. Induction of caspase-mediated cell death by matrix metalloproteinases in cerebral endothelial cells after hypoxia-reoxygenation. *J Cereb Blood Flow Metab*. 2004;24:720-727
38. Muneer PMA, Alikunju S, Szlachetka AM, Haorah J. The Mechanisms of Cerebral Vascular Dysfunction and Neuroinflammation by MMP-Mediated Degradation of VEGFR-2 in Alcohol Ingestion. *Arterioscler Thromb Vasc Biol*. 2012
39. Anea CB, Ali MI, Osmond JM, Sullivan JC, Stepp DW, Merloiu AM, Rudic RD. Matrix Metalloproteinase 2 and 9 Dysfunction Underlie Vascular Stiffness in Circadian Clock Mutant Mice. *Arterioscler Thromb Vasc Biol*. 2010;30:2535-2543
40. Gratchev A, Kzhyshkowska J, Kothe K, Muller-Molinet I, Kannookadan S, Utikal J, Goerdt S. Mphi1 and Mphi2 can be re-polarized by Th2 or Th1 cytokines, respectively, and respond to exogenous danger signals. *Immunobiology*. 2006;211:473-486
41. Mayer A, Lee S, Lendlein A, Jung F, Hiebl B. Efficacy of CD14+ blood monocytes/macrophages isolation: Positive versus negative MACS™ protocol. *Clin Hemorheol Microcirc*. 2011;48:57-63
42. Sharon JL, Puleo DA. Immobilization of glycoproteins, such as VEGF, on biodegradable substrates. *Acta Biomater*. 2008;4:1016-1023
43. Alberti K, Davey RE, Onishi K, George S, Salchert K, Seib FP, Bornhauser M, Pompe T, Nagy A, Werner C, Zandstra PW. Functional immobilization of signaling proteins enables control of stem cell fate. *Nat Meth*. 2008;5:645-650
44. Puccinelli TJ, Bertics PJ, Masters KS. Regulation of keratinocyte signaling and function via changes in epidermal growth factor presentation. *Acta Biomater*. 2010;6:3415-3425
45. Odedra D, Chiu LL, Shoichet M, Radisic M. Endothelial cells guided by immobilized gradients of vascular endothelial growth factor on porous collagen scaffolds. *Acta Biomater*. 2011;7:3027-3035
46. Gavard J, Gutkind JS. VEGF controls endothelial-cell permeability by promoting the beta-arrestin-dependent endocytosis of VE-cadherin. *Nat Cell Biol*. 2006;8:1223-1234
47. Reddy A, Sapp M, Feldman M, Subklewe M, Bhardwaj N. A monocyte conditioned medium is more effective than defined cytokines in mediating the terminal maturation of human dendritic cells. *Blood*. 1997;90:3640-3646
48. Hiebl B, Bog S, Mrowietz C, Juenger M, Jung F, Lendlein A, Franke RP. Influence of VEGF stimulated human macrophages on the proliferation of dermal microvascular endothelial cells: coculture experiments. *Clin Hemorheol Microcirc*. 2010;46:211-216
49. Moncada S, Gryglewski R, Bunting S, Vane JR. An enzyme isolated from arteries transforms prostaglandin endoperoxides to an unstable substance that inhibits platelet aggregation. *Nature*. 1976;263:663-665
50. Siess W, Roth P, Weber PC. Stimulated platelet aggregation, thromboxane B2 formation and platelet sensitivity to prostacyclin - a critical evaluation. *Thromb Haemost*. 1981;45:204-207
51. Cavalca V, Minardi F, Scurati S, Guidugli F, Squellerio I, Veglia F, Dainese L, Guarino A, Tremoli E, Caruso D. Simultaneous quantification of 8-iso-prostaglandin-F(2alpha) and 11-dehydro thromboxane B(2) in human urine by liquid chromatography-tandem mass spectrometry. *Anal Biochem*. 2010;397:168-174
52. Yoshizumi M, Abe J, Tsuchiya K, Berk BC, Tamaki T. Stress and vascular responses: atheroprotective effect of laminar fluid shear stress in endothelial cells: possible role of mitogen-activated protein kinases. *J Pharmacol Sci*. 2003;91:172-176
53. Gonzalez-Cabrero J, Pozo M, Duran MC, de Nicolas R, Egido J, Vivanco F. The proteome of endothelial cells. *Methods Mol Biol*. 2007;357:181-198

Figure 1. Viability, cell density and morpholpgy of adherent HUVEC mono-culture and HUVEC/aMO2 co-culture on cP*n*BA0250. A through R, representative images of HUVEC mono-cultures (A-C) and HUVEC/aMO2 co-cultures (D-F) seeded on elastic hydrophobic poly(*n*-butyl acrylate) networks with a Young's modulus of 250 kPa (cP*n*BA0250) for 3 h (A, D, G, J, M and P), for 24 h (B, E, H, K, N and Q) and 72 h (C, F, I, L, O and R). Fluoreszein diacetate (green) and propidium iodide (red) were used to visualise living cells and DNA of dead cells (A-F). F-actin cytoskeleton and nuclei of HUVEC mono-cultures (G-I) or HUVEC/aMO2 co-cultures (J-L) were stained after 3 h (G and J), 24 h (H and K) and 72 h (I and L) and CD14 mouse antihuman stained aMO2 green (P-R, white arrow). Cell densities as number of adherent cells per mm^2 (n_{ad}) were determined by enumerating nuclei of five fields of view per sample (n=6). Scale bar indicates 100 µm (A-L) or 50 µm (M-R).

Figure 2. HUVEC remain in their quiescent physiological status (A) mRNA expression of VEGF-A_{165} in HUVEC mono-culture and HUVEC/aMO2 co-culture relative to GAPDH on cP*n*BA0250. EC: HUVEC mono-culture, CO: HUVEC/aMO2 co-culture. Data represent mean of six experiments ± standard deviation. *p<0.05, **p<0.01 (B) MMP activity of HUVEC and aMO2. Supernatants were analysed for MMP activity by determining the increase in fluorescence intensity (FI) due to the cleavage of a MMP peptide substrate. On cP*n*BA0250 samples aMO2 mono-cultures, HUVEC mono-cultures and aMO2/HUVEC co-cultures were incubated for 24 h and 72 h. MO: aMO2 mono-culture, CO: HUVEC/aMO2 co-culture, EC: HUVEC mono-culture. Data represent mean of six experiments ± standard deviation. ***p<0.001

Figure 3. Distribution of adherent HUVEC on glass slides in mono-culture and HUVEC/aMO2 co-culture. HUVEC were cultured in regular EGM-2 (A), EGM-2 supplemented with 10 ng/ml VEGF-A_{165} (B), EGM-2 supplemented with 20 ng/ml VEGF-A_{165} (C) and co-cultured with aMO2 (D). After 6 days cells were stained for nuclei and F-actin skeleton. Fluorescently labeled F-actin is shown in red, nuclei are displayed in blue. Pictures represent one of three experiments. Scale bar indicates 100 µm.

Table 1. Cell densities of adherent cells in HUVEC mono-culture and HUVEC/aMO2 co-culture on glass slides after 1, 3, 6, 10, 14, 17 and 21 days. HUVEC were cultured either in EGM-2, EGM-2 supplemented with 10 ng/ml or 20 ng/ml VEGF-A_{165} or co-cultured with aMO2 in EGM-2. Data represents mean of three experiments ± standard deviation. One symbol: p<0.05, doubled symbol: p<0.01, + vs. aMO2, # vs. 10 ng/ml VEGF-A_{165}, ● vs. 20 ng/ml VEGF-A_{165}

Table 2. (A) Secretion of vasodilator prostacyclin (PGI2) and (B) vasoconstrictor thromboxane (TXB2) by HUVEC after 14 days of cultivation on glass slides in mono-culture and HUVEC/aMO2 co-culture. Concentration of prostacyclin c_{PGI2} and of thromboxane c_{TXB2} are given in pg/ml. Data represents mean of three experiments ± standard deviation. One symbol: p<0.05, doubled symbol: p<0.01, + vs. aMO2, # vs. 10 ng/ml VEGF-A_{165}, ● vs. 20 ng/ml VEGF-A_{165}.

Table 1

day	number of adherent cells per mm^2			
	EC + 0ng VEGF-A165	EC + 10ng VEGF-A165	EC + 20ng VEGF-A165	EC + aMO2
1	19 ± 6 $^{++,\bullet\bullet,\#\#}$	35 ± 13 $^{+,\bullet}$	48 ± 14	51 ± 16
3	64 ± 15 $^{++,\bullet\bullet,\#\#}$	100 ± 34	114 ± 36	112 ± 19
6	171 ± 29 $^{++}$	188 ± 51 $^{++}$	194 ± 65 $^{++}$	391 ± 68
10	183 ± 49 $^{++,\bullet\bullet,\#\#}$	279 ± 47 $^{++}$	304 ± 86 $^{++}$	464 ± 90
14	282 ± 71 $^{++,\bullet\bullet}$	330 ± 49 $^{++,\bullet\bullet}$	411 ± 40 $^{++}$	683 ± 107
17	418 ± 110 $^{\bullet}$	397 ± 105 $^{\bullet\bullet}$	523 ± 73	459 ± 77
21	306 ± 39 $^{++,\#\#}$	236 ± 43 $^{++,\bullet\bullet}$	344 ± 59 $^{++}$	596 ± 32

Table 2A

	c_{PGI2} in pg/ml			
day	EC + 0ng VEGF-A165	EC + 10ng VEGF-A165	EC + 20ng VEGF-A165	EC + aMO2
1	117 ± 8 $^{\#}$	214 ± 1	202 ± 51 $^{+}$	153 ± 39
3	125 ± 9 $^{\#}$	191 ± 22	186 ± 55	156 ± 35
6	71 ± 12 $^{\bullet\bullet}$	97 ± 11 $^{+}$	124 ± 7 $^{++}$	71 ± 7
10	94 ± 6	99 ± 9	116 ± 14	126 ± 23
14	319 ± 56 $^{\#,\bullet}$	91 ± 34 $^{++}$	131 ± 46	233 ± 18

Table 2B

	c_{TXB2} in pg/ml			
day	EC + 0ng VEGF-A165	EC + 10ng VEGF-A165	EC + 20ng VEGF-A165	EC + aMO2
1	13 ± 4 [#,+]	23 ± 1	27 ± 8	18 ± 3
3	16 ± 1 [#]	31 ± 6	31 ± 8	19 ± 7
6	31 ± 3	29 ± 6	39 ± 10	22 ± 11
10	53 ± 9 [#]	26 ± 3	37 ± 10	44 ± 6
14	78 ± 11 [#,•]	43 ± 14	52 ± 10	56 ± 7

Figure 1

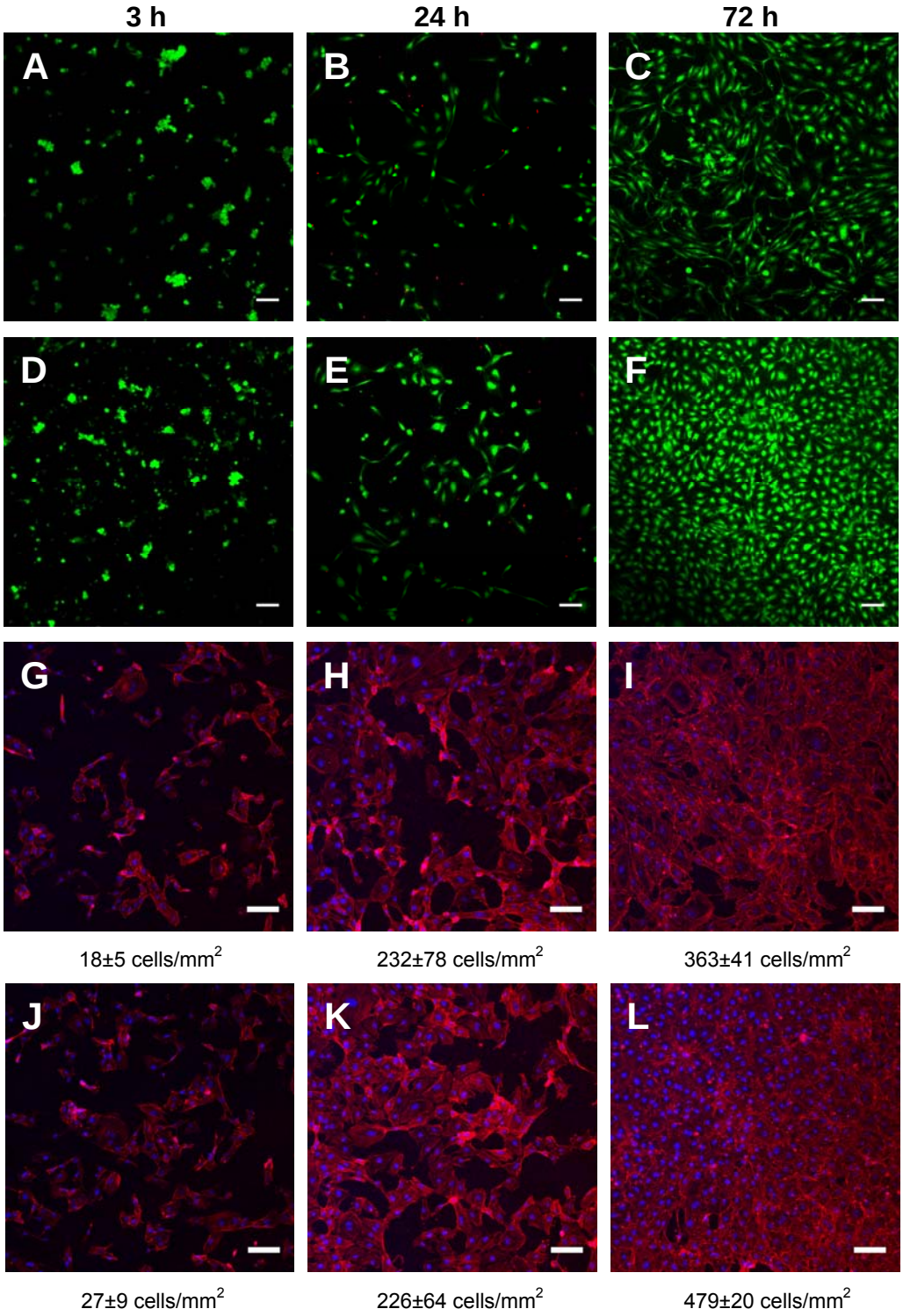
3 h
24 h
72 h
A
B
C
D
E
F
G
H
I
n_{ad}
18±5 cells/mm^2
232±78 cells/mm^2
363±41 cells/mm^2
J
K
L
n_{ad}
27±9 cells/mm^2
226±64 cells/mm^2
479±20 cells/mm^2

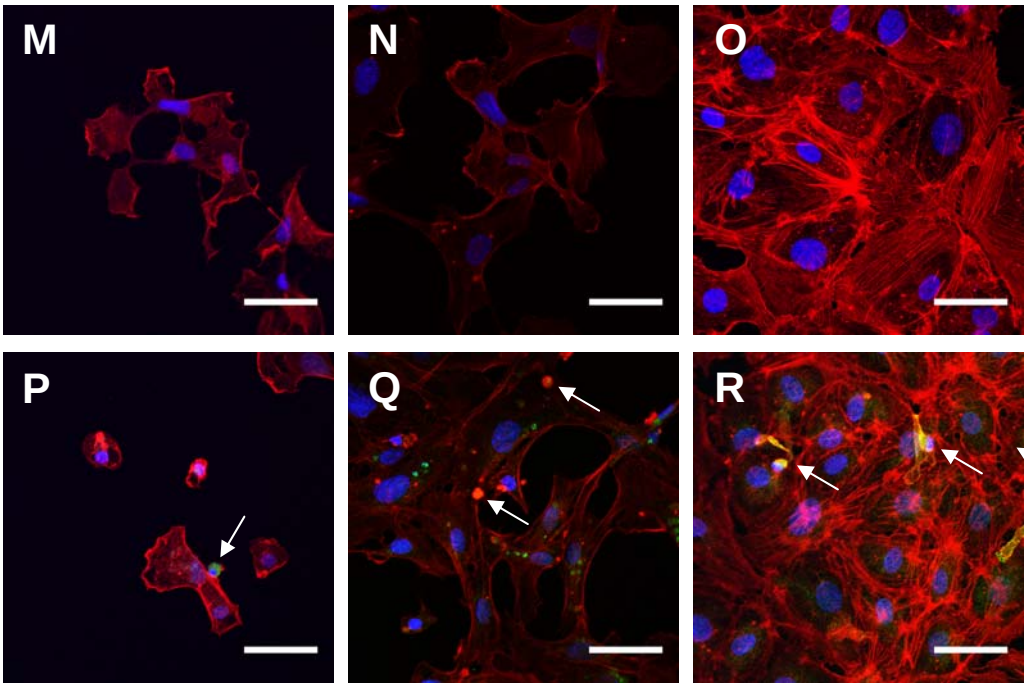
M
N
O
P
Q
R

Figure 2

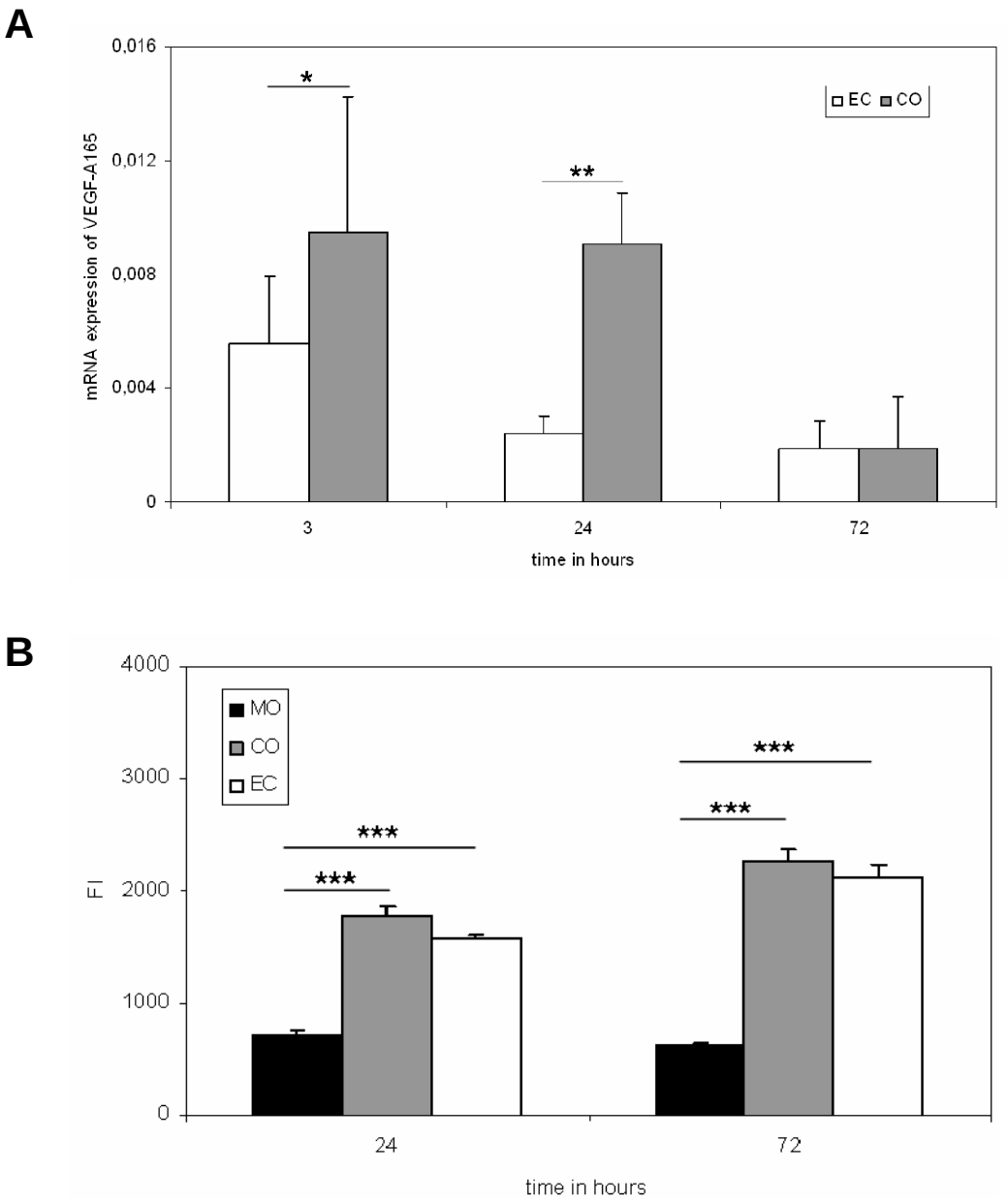
A
0,016
0,012
0,008
0,004
0
mRNA expression of VEGF-A165
*
**
EC
CO
3
24
72
time in hours
B
4000
3000
2000
1000
0
FI
MO
CO
EC
***
***
***
***
24
72
time in hours

Figure 3